Accelerated Publication

THE JOURNAL OF BIOLOGICAL CHEMISTRY
Vol. 279, No. 51, Issue of December 17, pp. 52816–52819, 2004

Crystal Structure of the Drug Discharge Outer Membrane Protein, OprM, of *Pseudomonas aeruginosa*

DUAL MODES OF MEMBRANE ANCHORING AND OCCLUDED CAVITY END*[S]

Received for publication, September 22, 2004,
and in revised form, October 14, 2004
Published, JBC Papers in Press, October 26, 2004,
DOI 10.1074/jbc.C400445200

Hiroyuki Akama‡, Misa Kanemaki‡, Masato Yoshimura§, Tomitake Tsukihara§, Tomoe Kashiwagi‡, Hiroshi Yoneyama‡, Shin-ichiro Narita‡, Atsushi Nakagawa§¶, and Taiji Nakae‡‖

From the ‡Department of Molecular Life Science, Tokai University School of Medicine, Isehara 259-1193, Japan and the §Institute for Protein Research, Osaka University, Suita 565-0871, Japan

The OprM lipoprotein of *Pseudomonas aeruginosa* is a member of the MexAB-OprM xenobiotic-antibiotic transporter subunits that is assumed to serve as the drug discharge duct across the outer membrane. The channel structure must differ from that of the porin-type open pore because the protein facilitates the exit of antibiotics but not the entry. For better understanding of the structure-function linkage of this important pump subunit, we studied the x-ray crystallographic structure of OprM at the 2.56-Å resolution. The overall structure exhibited trimeric assembly of the OprM monomer that consisted mainly of two domains: the membrane-anchoring β-barrel and the cavity-forming α-barrel. OprM anchors the outer membrane by two modes of membrane insertions. One is via the covalently attached NH_2-terminal fatty acids and the other is the β-barrel structure consensus on the outer membrane-spanning proteins. The β-barrel had a pore opening with a diameter of about 6–8 Å, which is not large enough to accommodate the exit of any antibiotics. The periplasmic α-barrel was about 100 Å long formed mainly by a bundle of α-helices that formed a solvent-filled cavity of about 25,000 Å^3. The proximal end of the cavity was tightly sealed, thereby not permitting the entry of any molecule. The result of this structure was that the resting state of OprM had a small outer membrane pore and a tightly closed periplasmic end, which sounds plausible because the protein should not allow free access of antibiotics. However, these observations raised another unsolved problem about the mechanism of opening of the OprM cavity ends. The crystal structure offers possible mechanisms of pore opening and pump assembly.

Infection of *Pseudomonas aeruginosa* is problematic in hospitals because the organism often infects immunocompromised patients and threatens their life. The underlying problem in the infection of this organism is that the bacterium shows both natural and mutational resistance to structurally and functionally dissimilar xenobiotics-antibiotics (1–4). This low specific antibiotic resistance is mainly attributable to the interplay of the multidrug exporter(s) and tight outer membrane barrier (5, 6).

P. aeruginosa encodes several resistance nodulation cell division-type transporters, and among them, the MexAB-OprM multidrug transporter plays a central role in intrinsic multidrug resistance of this organism (2, 7, 8). Upon mutation of the regulatory gene, *mexR*, the cell produces large amounts of MexAB-OprM rendering the bacterium severalfold more resistant to the same spectrum of antibiotics than the wild-type strain (4, 7, 8). The MexAB-OprM transporter consists of three subunit proteins, MexA, MexB, and OprM, located in the inner, inner, and the outer membrane, respectively (2, 9). MexB selects substrates and exports them by the expenditure of the energy of proton gradient across the cytoplasmic membrane (10). MexA, which is the inner membrane-anchored lipoprotein exposing the entire protein moiety to the periplasmic space, is assumed to cross-bridge the MexB and OprM subunits (3, 11). Recently, the crystal structure of the MexA subunit has been resolved at the 2.40-Å resolution, revealing that the long extended protein structure consists of three main domains and possibly one more disordered domain (12, 13). Based on the crystal structure of MexA and simulated MexB and OprM structures, the MexAB-OprM assembly model has been proposed.

OprM is the outer membrane-associated lipoprotein that is important in the final stage of antibiotic ejection across the outer membrane (9, 14). In fact, permeability measurements by means of a planar lipid bilayer and the liposome swelling assay reported that OprM forms the channel that allows the diffusion of small solutes (15, 16). The OprM protein lacking an amino-terminal cysteine residue and consequently lacking all of the fatty acids was predominantly recovered from the periplasmic space but only slightly recovered from the outer membrane fraction (14).

The TolC protein of *Escherichia coli* is a functional homologue of OprM in that the presence of TolC is a prerequisite for xenobiotic export by the AcrAB efflux pump, although the protein showed only 21% amino acid identity with OprM (15). The crystal structure of TolC had been resolved and the results revealed that the protein consisted mainly of two domains: one is the β-barrel structure by which the protein anchored the

* This work was supported in part by grants from the Ministry of Education, Culture, Sport, Science and Technology; by the 21st Century Centers of Excellence Research; by Protein 3000 project; and by Tokai University (Project Research Grant) and Tokai University School of Medicine (Research Project Grant). This work was performed under the Cooperative Research Program of Institute for Protein Research, Osaka University. The costs of publication of this article were defrayed in part by the payment of page charges. This article must therefore be hereby marked "*advertisement*" in accordance with 18 U.S.C. Section 1734 solely to indicate this fact.

[S] The on-line version of this article (available at http://www.jbc.org) contains the Experimental Procedures, supplemental Results, Table 1, and supplemental Figs. 1–4.

The atomic coordinates and structure factors (code 1WP1) have been deposited in the Protein Data Bank, Research Collaboratory for Structural Bioinformatics, Rutgers University, New Brunswick, NJ (http://www.rcsb.org/).

¶ To whom correspondence may be addressed. Tel./Fax: 81-6-6879-4313; E-mail: atsushi@protein.osaka-u.ac.jp.

‖ To whom correspondence may be addressed. Tel.: 81-463-93-5436; Fax: 81-463-93-5437; E-mail: nakae@is.icc.u-tokai.ac.jp.

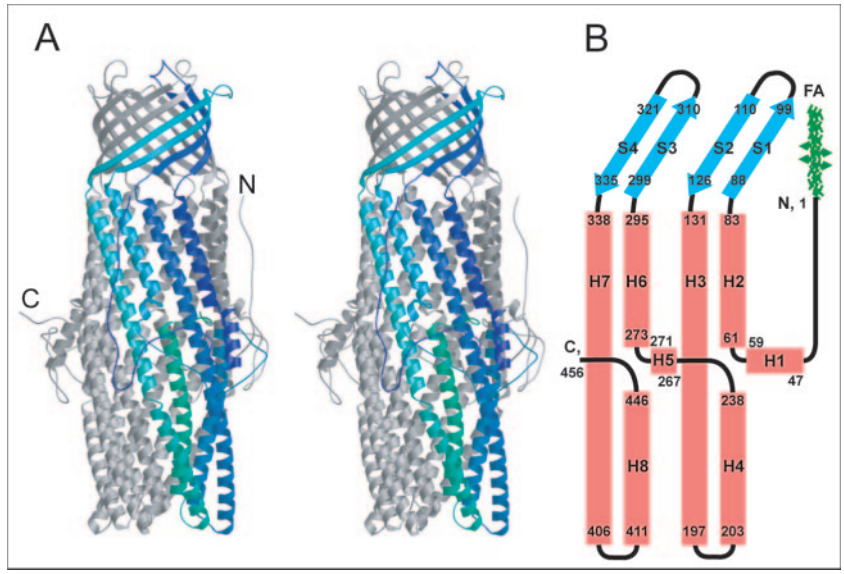

FIG. 1. **Stereoscopic view and secondary structure topology model of OprM.** *A*, stereoscopic view of the OprM trimer ribbon model. One monomer unit was distinguished from the other two with a blue and green. *B*, secondary structure topology model of the OprM monomer. The topology was constructed on the basis of the x-ray crystallographic structure of the molecule A, and secondary structure elements were defined by the DSSP program (28). The *arrows* and *box* represent the β-sheet and α-helix, respectively. *N* and *C* represent amino and carboxyl termini.

outer membrane and another is a long α-helical barrel that was extended to the periplasmic space (17). Both ends of TolC had a pore opening through which small solutes may diffuse. The OprM protein differs from TolC: (i) the amino-terminal end of the OprM was fatty acid modified (3, 14), whereas TolC has no such modification, and (ii) OprM functions only for xenobiotic discharge, while TolC is a multifunctional export protein engaged in protein export and small xenobiotic extrusion (18). To envisage the structure of this important transporter subunit and advance the understanding of how the pump assembly functions, we present the x-ray crystallographic structure of OprM.

EXPERIMENTAL PROCEDURES

All the materials used and experimental procedures are given in the supplemental materials section.

RESULTS AND DISCUSSION

Structure of the OpM Monomer—The mature form of OprM containing 468 amino acid residues and NH_2-terminal fatty acids was crystallized in the presence of a surfactant mixture, and diffraction data were obtained using synchrotron radiation. The current model of OprM consisted of 456 residues comprising 97.4% of the total amino acid residues. The OprM monomer consisted of four β-strands and eight α-helices (Fig. 1, *A* and *B*). β-Strands were organized in a single β-sheet cluster by the antiparallel configuration. The α-helix cluster mainly consisted of two long α-helices (67 and 69 residues) and four short helices (23 and 36 residues) with the anti-parallel configuration. Tandem joining of two short α-helices formed one set of α-helix similar in size and shape with a single long α-helix. The periplasmic end of the short α-helix H8 was buried in the two long α-helical ends. Assembly of two long α-helices and two sets of short α-helices per monomer were configured as if four long α-helices were in a bundle. The fatty acid-modified NH_2-terminal end was located at the interface of α-helix and β-sheet clusters near Phe^{297} and Phe^{129}.

The β-sheet and α-helix clusters were connected by four short loops consisting of two to four amino acid residues. There was a 110° turn at the junction of the β-strand and α-helix clusters, thereby changing their orientation toward the same direction and consequently forming a sickle shape. The aromatic amino acids, such as Phe^{85}, Phe^{129}, Phe^{296}, Phe^{297}, and Phe^{335}, at this region participated in the precise change of strand direction at the junctions, H2-S1, S2-H3, H6-S3, and S4-H7, respectively.

Overall Structure of the Trimer—Two OprM monomers were contained in cystallographic asymmetric unit and each monomers consisted trimeric structures, which were related crystallographic 3-fold (Fig. 1*A*). The overall structure is reminiscent of the TolC trimer of *E. coli* (17). Longitudinal and latitudinal dimensions of the OprM trimer appeared to be 135 and 40–75 Å, respectively. The trimer consisted mainly of two domains: a β-barrel with a size of about 35 (height) × 40–55 (width) Å and an α-barrel with a length of about 100 Å. Each β-sheet was tilted about 55° perpendicular to the plane of the membrane, twisted rightwards, and extending to two-thirds the distance along the β-barrel forming the barrel wall and a central pore. Near the top of the β-barrel, there were three short loops; they protruded toward the inside of the pore forming a constriction. The pore diameter was calculated to be about 6–8 Å at the constriction, which is much smaller than that of TolC (Fig. 2*A*). The β-barrel is likely inserted into the outer membrane matrix, analogous to the consensus β-barrel structure of most integral outer membrane proteins of Gram-negative bacteria (19). The surface of the β-barrel is hydrophobic and both ends of the β-barrel are positively charged (data not shown), and these electrostatic and hydrophobic features of the β-barrel strongly support the above hypothesis.

The α-barrel was formed by a bundle of 6 long α-helices and 12 short α-helices. Right-hand twists of α-helices toward the proximal ends narrowed the barrel end and spontaneously formed a bulge near the equator. Thus, the interior of the trimer formed a huge and long cavity along the longitudinal axis, with a volume of ~25,000 $Å^3$, which was probably filled with solvents. The cavity was gradually constricted along the proximal end and was totally closed at the tip (Fig. 2, *A* and *B*). This structure seems plausible, since the ground state of OprM should not allow access of xenobiotics to the interior of the cells.

Inlet and Outlet of the Cavity—The pore opening observed in the β-barrel with a diameter of about 6–8 Å, which is not large enough to accommodate the passage of any antibiotics (Fig. 2*A*). The periplasmic end of the α-barrel was tightly sealed, possibly not allowing the passage of any molecules in the ground state (Fig. 2, *A* and *B*).

A question to be answered is how the β-barrel pore can be dilated. The crystal structure showed two OprM molecules in different environment (Fig. 3*A*). Although all the amino acid residues in the β-barrel of the A unit could be traced, a large part of that of the B unit showed disordered structure (Fig. 3*A*). The results suggest that the upper part of the β-barrel is

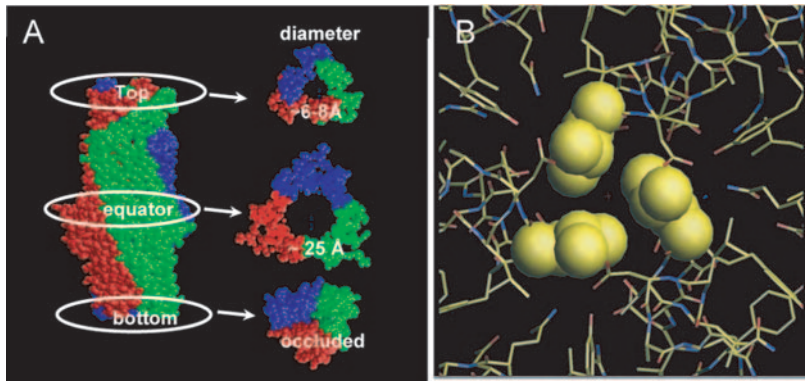

FIG. 2. **OprM cavity and the cavity ends.** *A*, vertical views and horizontal slices of the OprM trimer. Three monomers are colored *blue*, *red*, and *green*. The *left figure* shows a vertical view of the OprM trimer. The *right figures* exhibited horizontal slices of the OprM trimer at the β-barrel, equator, and the periplasmic end. Approximate pore diameters are shown. *B*, periplasmic end of the OprM trimer. Triplet Leu^{412} residues are shown by the space-filling model (*yellow*). The remaining amino acid residues are shown by a stick model.

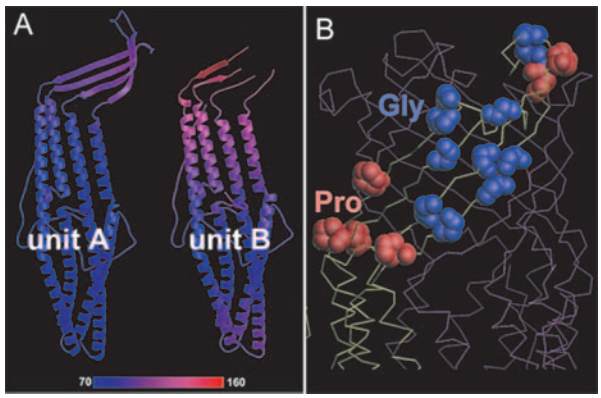

FIG. 3. **Comparison of asymmetric units A and B of the OprM monomer.** *A*, the ribbon model was drawn with a temperature factor in a gradient color. Note the disordered β-sheets at the *top* of the B unit and high temperature factors at the *top* and the *bottom*. *B*, localization of glycine and proline molecules in the β-barrel. The space-filling model was given only to one OprM. *Blue*, glycine; *red*, proline.

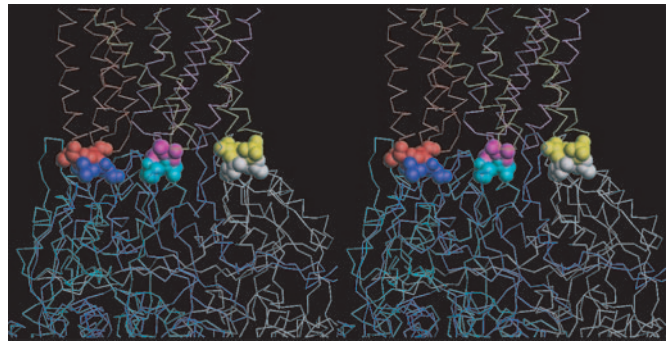

FIG. 4. **Stereoscopic view of the OprM-MexB junction.** Side view of the OprM-MexB junction in the trimeric form was shown. Arrays of hydrophobic amino acids, Val^{198}-Gly^{199}-Val^{200} of OprM (*red*, *magenta*, and *yellow*) and that of Ala^{736}-Leu^{737}-Gly^{738} of MexB (*blue*, *cyan*, and *white*) were shown by the space-filling model.

flexible. This assumption was supported by the fact that the β-barrel of one of the molecules in a crystal (molecule B in Fig. 3*A*) shows extremely high temperature factors (Fig. 3*A*). The β-barrel contained 18 residues of proline per trimer, which is known to have a tendency to break the protein secondary structure and 33 residues of glycine per trimer that confers fragility on the protein structure (Fig. 3*B*).

An even greater problem would be the periplasmic end of the α-barrel through which antibiotics may be injected into the OprM cavity. The α-helices at the periplasmic end were twisted causing closure of the cavity end. The gate was constructed by stacking of hydrophilic, hydrophobic, and hydrophilic amino acid networks (supplemental Fig. 1) that is flexible as shown by the high temperature factors (Fig. 3). The hydrophobic gate was formed by the triplet of Leu^{412} that may not allow the passage of even a water molecule (Fig. 2*B*). Two hydrophilic layers were constructed by Asp^{416}–Arg^{419} and Asn^{410}–Thr^{413} that sandwiched the hydrophobic layer (supplemental Fig. 1). This tightly sealed α-barrel end must be opened to allow the entry of antibiotics.

Proposal for the Mechanism of Opening the Closed Periplasmic End—The proximal end of the OprM α-barrel was tightly sealed by the inward twisting of helices 7 and 8, while helices 3 and 4 were positioned outside and interacted with MexB (Fig. 1*A*). This inward twisting seems to be maintained by strong intra- and intermolecular hydrogen bonding resulting in a turn of H7 and H8 at Gly^{377} and Val^{440}, respectively. If these turned α-helices could be linear, the periplasmic gate of the α-barrel could be opened. Hinges of this door are likely located near the equator of helices 7 and 8. The α-carbon of Arg^{376} and Gly^{377} of helix 7 and Glu^{439} and Val^{440} of helix 8 are aligned linearly; their 18° outward tilting at the hinges causes movement of the occluding Leu^{412} α-carbon 9.8 Å outward resulting in opening of a pore with a diameter of 11 Å or more (supplemental Fig. 4, movement of helices 7 and 8 of the *cyan* α-helices to the *magenta* α-helices). The model cannot predict the force that pulls out helices 7 and 8. Since OprM most likely interacts with MexB at the tip of helices 3 and 4, helices 7 and 8 are free from contact with MexB (see below). It is tempting to predict that this task may take place with the MexA subunit rather than MexB. A mechanism for the periplasmic pore dilation of the TolC trimer has been proposed that modification of the salt bridges at the tip of the periplasmic end enlarges the pore (20). However, the proposal did not consider possible involvement of the cognate subunit proteins such as AcrA and AcrB. The model proposed for pore opening of OprM is not mutually exclusive with that of TolC of *E. coli*. Further experimental data are needed to verify these models.

Membrane Anchoring—The amino-terminal cysteine residue of the OprM protein was fatty acid-modified. Removal of acyl chains had little effect on the function of OprM, although the majority of delipidated OprM had been recovered from the periplasmic space (14). Based on this result, we hypothesized that OprM might anchor the outer membrane solely via the acyl chains (14). However, the crystal structure did not support this conclusion and revealed that OprM anchors the outer membrane by two modes: via the NH_2-terminal fatty acids and the transmembrane β-barrel. The x-ray crystallography

showed a poorly resolved density map beyond the amino-terminal Cys[1] residue suggesting that this might be the fatty acid moiety (supplemental Fig. 2). The occurrence and structural clarification of a membrane protein that has two modes of membrane anchoring was a new finding to the best of our knowledge, although such a possibility was suggested in the outer membrane component of the capsular polysaccharide transport machinery in *E. coli* (21).

It would be of interest to address the physiological relevance of two modes of membrane anchoring. OprM has extremely large and hydrophilic surface areas, an external surface and internal cavity wall, which may need an additional membrane anchoring device to ensure transmembrane anchoring of the drug discharge duct (Fig. 2). This hypothesis was supported by the fact that the delipidated OprM was largely located in the periplasmic space (14) and by the structural fragility of the β-barrel (Fig. 3*B*). Alternatively, it is also possible that fatty acids play a role in the proper sorting of OprM to the outer membrane as documented in the *E. coli* Lol system (22). The fact that OprM lacks a carboxyl-terminal outer membrane sorting signal, *i.e.* Phe-*X*-Phe (COOH-terminal) (23), supports the above notion. However, TolC has neither a COOH-terminal outer membrane-sorting signal nor a NH_2-terminal fatty acid modification, yet the protein was properly sorted to the outer membrane.

Interaction of OprM with Cognate Subunits MexA and MexB—In vivo interaction of OprM with MexA and MexB has been demonstrated by co-purification of non-tagged MexA and MexB with his-tagged OprM (24) and by a chemical cross-linking experiment (25). Recently proposed MexAB-OprM assembly models showed that the coiled-coil domain of MexA interacts with OprM and both β- and $\alpha+\beta$-domains interact with MexB (12, 13). In fact, domain swapping experiments among *P. aeruginosa* membrane fusion protein revealed that the coiled-coil domain reserves the outer membrane selective determinant.[1] In addition, a genetic experiment revealed that function-restored secondary mutations that complement functionally compromised TolC *of E. coli* were predominantly mapped in the $\alpha+\beta$-domain of AcrA (26) suggesting that the $\alpha+\beta$-domain of AcrA may interact with TolC. Adopting these observations to explain the MexAB-OprM assembly, we revised the assembly model as follows. The OprM α-barrel provides at least two MexA binding sites: one for the coiled-coil α-helical domain and one for the $\alpha+\beta$-domain.

The next question for consideration is how OprM interacts with MexB. We constructed an OprM-MexB fitting model based on the OprM crystal structure and the simulated MexB model. The computer-aided manual search of close proximity and best fitting of the periplasmic end of the OprM to the distal end of the MexB funnel top found hydrophobic contact between these two subunits (Fig. 4). An array of hydrophobic amino acid residues of OprM, Val^{198}-Gly^{199}-Val^{200} (a loop between H3 and H4), provides perfect contact with an array of Ala^{736}-Leu^{737}-Gly^{738} of MexB (supplemental Fig. 3). Three hydrophobic contact sites in the OprM-MexB trimer strengthen the subunit interaction and contribute to the MexAB-OprM pump assembly. This contact may be maintained in either the closed or open state of the periplasmic end, because Val^{198}-Gly^{199}-Val^{200} is less likely to be involved in gate formation (supplemental Fig. 4). Arrays of hydrophobic amino acids found in OprM and MexB are also conserved in TolC and AcrB, respectively.

The MexA-MexB interaction is likely to occur at the disordered domain of MexA and the funnel domain of MexB. This assumption was supported by the earlier observation (25, 27). The remaining question is whether or not the 25 amino-terminal residues of MexA that are extended toward the outside of the $\alpha+\beta$-domain can reach the inner membrane. This short peptide consisted of a short β-sheet and a random coil that is most likely extended by a distance of about 50 Å toward the inner membrane and is long enough to reach the inner membrane. Fatty acids attached to this NH_2-terminal end must be inserted into the hydrophobic domain of the inner membrane.

Acknowledgments—We are grateful to the beam line staff member, E. Yamashita of SPing8 BL44XU, and Dr. H. Sakai of Osaka University for his advice in the initial stage of this study.

REFERENCES

1. Li, X. Z., Nikaido, H., and Poole, K. (1995) *Antimicrob. Agents Chemother.* **39,** 1948–1953
2. Morshed, S. R., Lei, Y., Yoneyama, H., and Nakae, T. (1995) *Biochem. Biophys. Res. Commun.* **210,** 356–362
3. Poole, K., Heinrichs, D. E., and Neshat, S. (1993) *Mol. Microbiol.* **10,** 529–544
4. Rella, M., and Haas, D. (1982) *Antimicrob. Agents Chemother.* **22,** 242–249
5. Nikaido, H. (1996) *Science* **264,** 221–229
6. Nakae, T. (1995) *Microbiol. Immunol.* **39,** 221–229
7. Srikumar, R., Paul, C. J., and Poole, K. (2000) *J. Bacteriol.* **182,** 1410–1414
8. Saito, K., Yoneyama, H., and Nakae, T. (1999) *FEMS Microbiol. Lett.* **179,** 67–72
9. Poole, K., Krebes, K., McNally, C., and Neshat, S. (1993) *J. Bacteriol.* **175,** 7363–7372
10. Lei, Y., Sato, K., and Nakae, T. (1991) *Biochem. Biophys. Res. Commun.* **178,** 1043–1048
11. Yoneyama, H., Maseda, H., Kamiguchi, H., and Nakae, T. (2000) *J. Biol. Chem.* **275,** 4628–4634
12. Akama, H., Matsuura, T., Kashiwagi, S., Yoneyama, H., Tsukihara, T., Nakagawa, A., Narita, S.-I., and Nakae, T. (2004) *J. Biol. Chem.* **279,** 25939–25942
13. Higgins, M. K., Bokma, E., Koronakis, E., Hughes, C., and Koronakis, V. (2004) *Proc. Natl. Acad. Sci. U. S. A.* **101,** 9994–9999
14. Nakajima, A., Sugimoto, Y., Yoneyama, H., and Nakae, T. (2000) *J. Biol. Chem.* **275,** 30064–30068
15. Wong, K. K. Y., Brinkman, F. S. L., Benz, R. S., and Hancock, R. E. W. (2001) *J. Bacteriol.* **183,** 367–374
16. Yoshihara, E., Maseda, H., and Saito, K. (2002) *Eur. J. Biochem.* **269,** 4738–4745
17. Koronakis, V., Sharff, A., Koronakis, E., Luisi, B., and Hughes, C. (2000) *Nature* **405,** 914–919
18. Paulsen, I. T., Park, J. H., Choi, P. S., and Saier MH, J. r. (1997) *FEMS Microbiol. Lett.* **156,** 1–8
19. Wimley, W. C. (2003) *Curr. Opin. Struct. Biol.* **13,** 404–411
20. Andersen, C., Bokma, E., Eswaran, J., Humphreys, D., Hughes, C., and Koronakis, V. (2002) *Proc. Natl. Acad. Sci. U. S. A.* **99,** 11103–11108
21. Drummelsmith, J., and Whitfield, C. (2000) *EMBO J.* **19,** 57–66
22. Yakushi, T., Masuda, K., Narita, s., Matsuyama, S., and Tokuda, H. (2000) *Nature Cell Biol.* **2,** 212–218
23. Struyve, M., Moons, M., and Tommassen, J. (1991) *J. Mol. Biol.* **218,** 141–148
24. Mokhonov, V. V., Mokhonova, E. I., Akama, H., and Nakae, T. (2004) *Biochem. Biophys. Res. Commun.* **322,** 483–489
25. Nehme, D., Li, X. Z., Elliot, R., and Poole, K. (2004) *J. Bacteriol.* **186,** 2973–2983
26. Gerken, H., and Misra, R. (2004) *Mol. Microbiol.* **54,** 620–631
27. Elkins, C. A., and Nikaido, H. (2003) *J. Bacteriol.* **185,** 5349–5356
28. Kabsch, W., and Sander, C. (1983) *Biopolymers* **22,** 2577–2637

[1] S. Eda and T. Nakae, manuscript in preparation.

Crystal Structure of the Drug Discharge Outer Membrane Protein, OprM, of *Pseudomonas aeruginosa*: DUAL MODES OF MEMBRANE ANCHORING AND OCCLUDED CAVITY END

Hiroyuki Akama, Misa Kanemaki, Masato Yoshimura, Tomitake Tsukihara, Tomoe Kashiwagi, Hiroshi Yoneyama, Shin-ichiro Narita, Atsushi Nakagawa and Taiji Nakae

J. Biol. Chem. 2004, 279:52816-52819.
doi: 10.1074/jbc.C400445200 originally published online October 26, 2004